

RESEARCH PAPER



# Discovery of triterpenoids as potent dual inhibitors of pancreatic lipase and human carboxylesterase 1

Jing Zhang<sup>a\*</sup>, Qiu-Sha Pan<sup>a\*</sup>, Xing-Kai Qian<sup>a,b</sup>, Xiang-Lu Zhou<sup>a</sup>, Ya-Jie Wang<sup>a</sup>, Rong-Jing He<sup>a</sup>, Le-Tian Wang<sup>a</sup>, Yan-Ran Li<sup>a</sup>, Hong Huo<sup>c</sup>, Cheng-Gong Sun<sup>d</sup>, Lei Sun<sup>d</sup>, Li-Wei Zou<sup>a</sup> and Ling Yang<sup>a</sup>

<sup>a</sup>Institute of Interdisciplinary Integrative Medicine Research, Shanghai University of Traditional Chinese Medicine, Shanghai, China; <sup>b</sup>Translational Medicine Research Center, Guizhou Medical University, Guizhou, China; <sup>c</sup>Dalian Institute of Chemical Physics, Chinese Academy of Sciences, Dalian, China; <sup>d</sup>The Second Hospital of Dalian Medical University, Dalian, China

## ABSTRACT

Pancreatic lipase (PL) is a well-known key target for the prevention and treatment of obesity. Human carboxylesterase 1A (hCES1A) has become an important target for the treatment of hyperlipidaemia. Thus, the discovery of potent dual-target inhibitors based on PL and hCES1A hold great potential for the development of remedies for treating related metabolic diseases. In this study, a series of natural triterpenoids were collected and the inhibitory effects of these triterpenoids on PL and hCES1A were determined using fluorescence-based biochemical assays. It was found that oleanolic acid (OA) and ursolic acid (UA) have the excellent inhibitory effects against PL and hCES1A, and highly selectivity over hCES2A. Subsequently, a number of compounds based on the OA and UA skeletons were synthesised and evaluated. Structure–activity relationship (SAR) analysis of these compounds revealed that the acetyl group at the C-3 site of UA (compound **41**) was very essential for both PL and hCES1A inhibition, with IC<sub>50</sub> of 0.75 μM and 0.014 μM, respectively. In addition, compound **39** with 2-enol and 3-ketal moiety of OA also has strong inhibitory effects against both PL and hCES1A, with IC<sub>50</sub> of 2.13 μM and 0.055 μM, respectively. Furthermore, compound **39** and **41** exhibited good selectivity over other human serine hydrolases including hCES2A, butyrylcholinesterase (BChE) and dipeptidyl peptidase IV (DPP-IV). Inhibitory kinetics and molecular docking studies demonstrated that both compounds **39** and **41** were effective mixed inhibitors of PL, while competitive inhibitors of hCES1A. Further investigations demonstrated that both compounds **39** and **41** could inhibit adipocyte adipogenesis induced by mouse preadipocytes. Collectively, we found two triterpenoid derivatives with strong inhibitory ability on both PL and hCES1A, which can be served as promising lead compounds for the development of more potent dual-target inhibitors targeting on PL and hCES1A.

## ARTICLE HISTORY

Received 4 November 2021  
Revised 28 December 2021  
Accepted 11 January 2022

## KEYWORDS

Triterpenoids; pancreatic lipase; human carboxylesterase 1; dual inhibitors; adipocyte adipogenesis

## 1. Introduction

The morbidity and mortality of metabolic diseases such as hyperlipidaemia and diabetes are increasing year by year in developed and developing countries, which is inseparable from the changes in modern lifestyles and the increase in consumption of high-sugar and high-fat diets<sup>1–3</sup>. Studies have shown that elevated levels of fatty acids, cholesterol and other esters are important risk factors for metabolic diseases such as hypertension, arteriosclerosis, non-alcoholic fat, and type II diabetes<sup>4,5</sup>. Therefore, around the key targets of lipids, effective drugs that regulate lipid metabolism are an important direction for treating metabolic diseases and revealing the mechanism of metabolic diseases.

Mammalian carboxylesterase (CEs) is an important phase I metabolic enzyme, which is related to the metabolism or detoxification of endogenous substances, clinical drugs and environmental toxicants, and participates in a large number of ester drugs and other biotransformation and metabolic clearance of non-drug

exogenous ester compounds<sup>6–10</sup>. Human carboxylesterase 1A (hCES1A) and human carboxylesterase 2A (hCES2A) are the two main subtypes in the human body. Although the amino acid sequences of hCES1A and hCES2A share 47% homology, there are significant differences in tissue distribution and substrate selectivity<sup>9,11–13</sup>. hCES1A is highly expressed in the liver, but relatively low in intestine and kidney. The preferred substrates of hCES1A are those compounds with relatively larger acyl groups and smaller alcohol structures, such as clopidogrel and oseltamivir<sup>14,15</sup>. In contrast, hCES2A is mainly distributed in the gastrointestinal tract, especially in the small intestine. Compounds containing smaller acyl groups and larger alcohol groups tend to be hydrolysed by hCES2A, such as irinotecan, capecitabine and flutamide<sup>16,17</sup>.

As an important serine hydrolases with the abundant distribution in the human hepatocytes and adipocytes, hCES1A plays a critical role in the hydrolysis of a large number of endogenous esters such as triglycerides and cholesteryl esters, so as to

**CONTACT** Li-Wei Zou  [chemzlw@163.com](mailto:chemzlw@163.com)  Institute of Interdisciplinary Integrative Medicine Research, Shanghai University of Traditional Chinese Medicine, Shanghai 201203, China; Lei Sun  [417186487@qq.com](mailto:417186487@qq.com)  The Second Hospital of Dalian Medical University, Dalian 116023, China

\*These authors contributed equally to this work.

 Supplemental data for this article can be accessed [here](#).

© 2022 The Author(s). Published by Informa UK Limited, trading as Taylor & Francis Group.

This is an Open Access article distributed under the terms of the Creative Commons Attribution License (<http://creativecommons.org/licenses/by/4.0/>), which permits unrestricted use, distribution, and reproduction in any medium, provided the original work is properly cited.

participate in physiological and pathological processes, such as cholesterol homeostasis, lipid metabolism and fatty liver<sup>18,19</sup>. Studies have shown that knocking out mice's carboxylesterase 3 (Ces3, homologous to human hCES1A) will cause a significant decrease in plasma triglyceride and apolipoprotein B levels<sup>20</sup>. Meanwhile, the deficiency of Ces3 nullified the browning effect in white adipocytes, along with reduced adipogenesis in 3T3-L1 adipocytes<sup>21</sup>. In addition, a number of studies have shown that hCES1A expression is positively correlated with obesity, and its expression is up-regulated in fat cells in obese and type 2 diabetes patients<sup>18,22,23</sup>. Due to the key roles of hCES1A responsible for the enzymatic cleaving of triglyceride stores in hepatocytes, it has become an important target for the treatment of hypertriglyceridaemia<sup>24–26</sup>.

As the key enzyme of triglyceride hydrolysis in the intestine, pancreatic lipase (PL) catalyses the hydrolysis of the ester bond of triacylglycerols to monoacylglycerols and fatty acids, and contributes to 50–70% hydrolysis of total dietary fats<sup>27,28</sup>. Inhibition of PL activity could restrain the hydrolysis of dietary glycerides in food, so as to reduce the subsequent absorption of free fatty acids and monoacylglycerols. Therefore, PL has become a promising target for the adjuvant treatment of obesity and hypertriglyceridaemia<sup>29,30</sup>. In addition, inhibiting the activity of hCES1A could display multiple beneficial effects in both lipid and glucose homeostasis in genetic and diet-induced mouse models of obesity, insulin resistance and type 2 diabetes<sup>18</sup>. Thus, the discovery of potent dual-target inhibitors based on hCES1A and PL hold great potential for the development of remedies for treating related metabolic diseases such as hypertriglyceridaemia and obesity. However, the development of dual target inhibitors of hCES1A and PL is still in the blank stage.

To date, pharmaceutical chemists have found most CES inhibitors with good inhibitory activity. However, most of them are identified as potent and selective inhibitors against hCES2A. hCES1A inhibitors with high potency and selectivity are rarely reported, and their inhibitory activities to PL are not investigated<sup>31–33</sup>. At present, only GR148672x, a hCES1A inhibitor developed by GlaxoSmithKline, has entered the preclinical research stage, but its subtype selectivity data has not been disclosed<sup>26</sup>. Orlistat, a PL inhibitor, developed by Roche for the treatment of obesity and marketed as a prescription drug in New Zealand in 1998<sup>34</sup>. At present, orlistat remains the only PL inhibitor approved by the Food and Drug Administration (FDA) for obesity management. However, due to the non-negligible adverse effects, including oil stool, diarrhoea, fat-soluble vitamin deficiencies and hepatotoxicity, orlistat's application has been limited<sup>35,36</sup>. Thus, it is highly desirable to find potent dual inhibitors targeting hCES1A and PL for the prevention and treatment of related metabolic diseases.

Triterpenoids, structurally diverse natural products, are widely distributed in various parts of plant including seeds, roots, flowers, leaves and fruits<sup>37,38</sup>. In the past decade, triterpenoids have been used as an effective structural template to find more effective lead compounds with a variety of pharmacological properties<sup>39</sup>, such as anti-tumour<sup>40</sup>, anti-virus<sup>41</sup>, anti-diabetes<sup>42</sup>, kidney-protective activity<sup>43</sup>, etc.

In this study, a series of triterpenoids were collected and the inhibitory effects of these triterpenoids on PL were assayed using 4-methylumbelliferyl oleate (4-MUO) as substrate probe<sup>44</sup>. After preliminary screening, we found that nine triterpenoids displayed good inhibitory effects against PL. More in-depth researches on the inhibitory effects of these nine triterpenoids against CES were assayed using *N*-alkylated  $\rho$ -luciferin methyl ester (NLMe) and

fluorescent diacetate (FD) as specific optical substrate for hCES1A, and hCES2A, respectively. It was found that the ursolic acid (UA) and oleanolic acid (OA) have an excellent inhibitory effect on hCES1A and highly selectivity over hCES2A. Thus, we select UA and OA as the scaffolds and focus on their structural modifications to design and synthesise a batch of compounds to obtain potent dual target inhibitors of hCES1A and PL.

## 2. Experimental

### 2.1. Chemicals and reagents

Oleanolic acid, maslinic acid, hederagenin, ursolic acid, corosolic acid, asiatic acid,  $\beta$ -boswellic acid, glycyrrhetic acid, celastrol, betulin, betulinicaldehyde, betulinic acid, pachymic acid, ganoderic acid B, polygalacic acid, glycyrrhizic acid, lupeol, ginsenosideol F1, ginsenoside Rg1, ginsenoside Rg2, were purchased from Dalian Meilun Company (Beijing, China), ginsenoside Rd, ginsenoside R1, Notoginsenoside R1 were purchased from Sichuan Weikeqi Biotechnology Co., Ltd. (Chengdu, China), ginsenoside Re, ginsenoside Rh1 were purchased from Chengdu Pfeid Biotech Technology Co., Ltd. (Chengdu, China), ginsenoside Ro, ginsenoside Rh4, and ginsenoside F4 were purchased from Chenguang Bio (Handan, China). Fluorescent diacetate (FD, a fluorescent substrate for hCES2A) was purchased from TCI (Tokyo, Japan). Pancreatic lipase (PL, type II, Lot.SLBN9099V; EC 3.1.1.3), 4-methylumbelliferone (4-MU) were purchased from Sigma Aldrich (St. Louis, MO). 4-Methylumbelliferyl oleate (4-MUO) was obtained from J&K chemical (Beijing, China) as PL fluorescent substrate. NLMe was independently developed and synthesised by the laboratory, stored at  $-20^{\circ}\text{C}$  refrigerator [45]. Luciferin detection reagent (LDR) was purchased from Promega Biotech (Madison, WI). The pooled human liver microsomes from 50 donors (HLM, lot No. X008067) were purchased from Bioreclamation IVT (Baltimore, MD). 0.1 M McIlvane buffer (0.1 M citrate- $\text{Na}_2\text{HPO}_4$ , pH 7.4) and 0.1 M phosphate buffered saline (PBS, pH 6.5 and 7.4) were prepared by using Milli-Q Water (Millipore, Bedford, CA). Bis-p-nitrophenyl phosphate (BNPP) was purchased from TCI (Tokyo, Japan). LC grade dimethyl sulfoxide (DMSO, Tedia, Fairfield, OH) was used as the stock solution of the compound and then stored at  $4^{\circ}\text{C}$  until use. The stock solution of enzyme substrate (100 mM) was dissolved in dimethyl sulfoxide and stored at  $-20^{\circ}\text{C}$ .  $^1\text{H}$  NMR and  $^{13}\text{C}$  NMR spectra were recorded using Bruker Avance II (600 MHz) spectrometer with chemical shifts reported as ppm (in DMSO- $d_6$  or  $\text{CDCl}_3$ , TMS as an internal standard). High-resolution MS data were recorded with the 5600 Triple TOF quadrupole-time-of-flight mass spectrometer.

### 2.2. Synthesis of OA and UA derivatives

See the Supporting Information for more details.

Compound **30**, white solid,  $^1\text{H}$  NMR (600 MHz, DMSO)  $\delta$  12.05 (s, 1H), 5.19 (t,  $J=3.4$  Hz, 1H), 2.76 (dd,  $J=13.8, 4.1$  Hz, 1H), 2.55–2.46 (m, 1H), 2.32–2.27 (m, 1H), 2.00–1.81 (m, 3H), 1.77–1.75 (, 1H), 1.72–1.56 (m, 4H), 1.53–1.37 (m, 6H), 1.35–1.23 (m, 3H), 1.50–1.11 (m, 4H), 1.09–1.01 (m, 2H), 1.01–0.93 (t, 9H), 0.86 (d, 6H), 0.77 (s, 3H).  $^{13}\text{C}$  NMR (151 MHz, DMSO)  $\delta$  216.66, 179.05, 144.29, 121.88, 54.75, 47.09, 46.61, 46.11, 45.96, 41.93, 41.37, 39.29, 38.86, 34.12, 33.79, 33.28, 32.53, 32.29, 30.87, 27.69, 26.75, 25.94, 23.82, 23.45, 23.10, 21.58, 19.61, 17.16, 15.16. LC/MS (ESI): Calcd. for  $\text{C}_{30}\text{H}_{45}\text{O}_3^-$  ( $[\text{M}-\text{H}]^-$ ) 453.3, Found. 453.3.

Compound **31**, white solid,  $^1\text{H}$  NMR (600 MHz, DMSO)  $\delta$  11.91 (s, 1H), 5.10 (s, 1H), 4.33 (m, 1H), 2.72–2.61 (m, 1H), 1.93 (s, 3H),

1.92–1.80 (m, 1H), 1.76–1.74 (m, 2H), 1.67–1.33 (m, 12H), 1.33–1.23 (m, 2H), 1.21–1.08 (m, 2H), 1.04 (s, 3H), 1.02–0.88 (m, 3H), 0.83–0.81 (m, 9H), 0.75 (s, 6H), 0.66 (s, 3H).  $^{13}\text{C}$  NMR (151 MHz, DMSO)  $\delta$  179.05, 170.61, 144.32, 121.87, 80.38, 54.99, 47.72, 47.31, 46.14, 45.92, 41.81, 41.27, 38.00, 37.71, 36.96, 33.77, 33.28, 33.02, 32.69, 32.54, 31.44, 30.86, 30.75, 28.23, 27.67, 26.01, 25.80, 23.84, 23.66, 23.35, 23.07, 22.68, 21.44, 18.25, 17.28, 17.10, 15.52. LC/MS (ESI): Calcd. for  $\text{C}_{32}\text{H}_{49}\text{O}_4^-$  ( $[\text{M}-\text{H}]^-$ ) 497.3, Found. 497.3.

Compound **32**, white solid,  $^1\text{H}$  NMR (600 MHz, DMSO)  $\delta$  6.77 (d,  $J=13.4$  Hz, 2H), 5.21 (s, 1H), 4.39 (dd,  $J=11.7$ , 4.4 Hz, 1H), 2.74 (dd,  $J=13.3$ , 3.6 Hz, 1H), 2.00 (s, 3H), 1.89–1.86 (m, 1H), 1.81 (dd,  $J=8.6$ , 3.0 Hz, 2H), 1.72–1.35 (m, 12H), 1.35–1.17 (m, 3H), 1.10 (s, 3H), 1.09–0.91 (m, 4H), 0.87 (t, 9H), 0.81 (d, 6H), 0.72 (s, 3H).  $^{13}\text{C}$  NMR (151 MHz, DMSO)  $\delta$  179.26, 170.60, 144.72, 121.63, 80.39, 55.01, 47.34, 46.60, 45.66, 41.77, 40.98, 39.31, 38.01, 37.71, 36.96, 34.13, 33.40, 33.08, 32.74, 30.91, 28.24, 27.49, 26.05, 23.99, 23.67, 23.35, 22.84, 21.44, 18.27, 17.37, 17.10, 15.53. LC/MS (ESI): Calcd. For  $\text{C}_{32}\text{H}_{52}\text{NO}_3^+$  ( $[\text{M}+\text{H}]^+$ ) 498.4, Found. 498.4.

Compound **33**, white solid,  $^1\text{H}$  NMR (600 MHz, DMSO)  $\delta$  12.13 (bs, 1H), 5.16 (t,  $J=3.3$  Hz, 1H), 4.41 (dd,  $J=11.7$ , 4.5 Hz, 1H), 2.74 (dd,  $J=13.8$ , 4.1 Hz, 1H), 2.50–2.45 (m, 4H), 2.42 (s, 3H), 1.94–1.89 (m, 1H), 1.83–1.81 (m, 2H), 1.70–1.42 (m, 1H), 1.38–1.13 (m, 4H), 1.11 (s, 3H), 1.09–0.96 (m, 3H), 0.88 (d, 9H), 0.81 (s, 6H), 0.72 (s, 3H).  $^{13}\text{C}$  NMR (151 MHz, DMSO)  $\delta$  179.04, 174.05, 173.87, 172.09, 144.33, 121.88, 80.47, 55.01, 47.29, 46.13, 45.92, 41.81, 41.27, 39.57, 39.33, 37.95, 37.79, 36.95, 33.77, 33.28, 32.69, 32.55, 30.86, 29.65, 29.25, 28.17, 27.67, 26.03, 23.84, 23.61, 23.35, 23.07, 18.25, 17.28, 17.08, 15.50. LC/MS (ESI): Calcd. For  $\text{C}_{34}\text{H}_{51}\text{O}_6^-$  ( $[\text{M}-\text{H}]^-$ ) 555.3, Found. 555.3.

Compound **34**, white solid,  $^1\text{H}$  NMR (600 MHz,  $\text{CDCl}_3$ )  $\delta$  5.28 (t,  $J=3.4$  Hz, 1H), 4.52–4.49 (m, 1H), 4.50 (dd,  $J=9.8$ , 6.1 Hz, 1H), 2.83–2.80 (m, 1H), 2.32–2.24 (m, 2H), 2.01–1.96 (m, 1H), 1.93–1.84 (m, 2H), 1.81–1.69 (m, 2H), 1.69–1.49 (m, 11H), 1.47–1.40 (m, 2H), 2.06–0.60 (m, 53H), 1.36–1.27 (m, 2H), 1.24–1.15 (m, 2H), 1.14 (s, 3H), 1.09–1.04 (m, 2H), 0.98–0.92 (m, 9H), 0.90 (s, 3H), 0.86 (d, 6H), 0.75 (s, 3H).  $^{13}\text{C}$  NMR (151 MHz,  $\text{CDCl}_3$ )  $\delta$  183.46, 173.53, 143.59, 122.58, 80.56, 55.30, 47.54, 46.53, 45.84, 41.57, 40.95, 39.28, 38.06, 37.73, 36.99, 36.77, 33.79, 33.05, 32.54, 32.43, 30.67, 28.05, 27.67, 25.90, 23.57, 23.40, 22.90, 18.65, 18.17, 17.16, 16.71, 15.37, 13.73. LC/MS (ESI): Calcd. for  $\text{C}_{34}\text{H}_{53}\text{O}_4^-$  ( $[\text{M}-\text{H}]^-$ ) 525.4, Found. 525.4.

Compound **35**, white solid,  $^1\text{H}$  NMR (600 MHz,  $\text{CDCl}_3$ )  $\delta$  5.27 (t,  $J=3.4$  Hz, 1H), 4.51–4.49 (m, 1H), 2.83–2.80 (m, 1H), 2.35–2.24 (m, 2H), 2.01–1.96 (m, 1H), 1.94–1.84 (m, 2H), 1.80–1.68 (m, 2H), 1.68–1.52 (m, 10H), 1.51–1.38 (m, 2H), 1.38–1.23 (m, 7H), 1.23–1.11 (m, 5H), 1.10–1.02 (m, 2H), 0.96–0.88 (m, 12H), 0.86 (d,  $J=5.4$  Hz, 6H), 0.75 (s, 3H).  $^{13}\text{C}$  NMR (151 MHz,  $\text{CDCl}_3$ )  $\delta$  183.77, 173.71, 143.59, 122.58, 80.56, 55.29, 47.54, 46.54, 45.83, 41.56, 40.93, 39.28, 38.05, 37.73, 36.99, 34.82, 33.78, 33.06, 32.53, 32.43, 31.35, 30.67, 28.05, 27.66, 25.91, 24.84, 23.57, 23.56, 23.39, 22.89, 22.32, 18.17, 17.16, 16.72, 15.37, 13.92. LC/MS (ESI): Calcd. for  $\text{C}_{36}\text{H}_{57}\text{O}_4^-$  ( $[\text{M}-\text{H}]^-$ ) 553.4, Found. 553.4.

Compound **36**, white solid,  $^1\text{H}$  NMR (600 MHz, DMSO)  $\delta$  5.18 (s, 1H), 4.29 (d,  $J=5.2$  Hz, 1H), 3.54 (s, 3H), 3.01–2.97 (m, 1H), 2.79–2.76 (m, 1H), 2.05–1.91 (m, 1H), 1.89–1.72 (m, 2H), 1.65–1.56 (m, 2H), 1.55–1.28 (m, 11H), 1.25–1.12 (m, 2H), 1.08 (m, 3H), 1.08–0.90 (m, 3H), 0.88 (d, 9H), 0.85 (s, 3H), 0.68 (s, 3H), 0.65 (s, 3H).  $^{13}\text{C}$  NMR (151 MHz, DMSO)  $\delta$  177.62, 143.92, 122.32, 77.27, 55.23, 51.90, 47.50, 46.51, 45.86, 41.66, 41.36, 39.27, 38.84, 38.50, 37.03, 33.61, 33.21, 32.74, 32.46, 30.82, 28.67, 27.62, 27.40, 26.12, 23.82, 23.36, 23.06, 18.44, 17.02, 16.48, 15.53. LC/MS (ESI): Calcd. for  $\text{C}_{31}\text{H}_{51}\text{O}_3^+$  ( $[\text{M}+\text{H}]^+$ ) 471.4, Found. 471.4.

Compound **37**, white solid,  $^1\text{H}$  NMR (600 MHz,  $\text{CDCl}_3$ )  $\delta$  5.19 (t,  $J=3.5$  Hz, 1H), 3.55 (d,  $J=10.9$  Hz, 1H), 3.22 (dd,  $J=11.2$ , 4.0 Hz,

2H), 1.98 (dd,  $J=13.6$ , 4.2 Hz, 1H), 1.90–1.85 (m, 3H), 1.77–1.69 (m, 2H), 1.65–1.53 (m, 6H), 1.51–1.39 (m, 7H), 1.36–1.28 (m, 3H), 1.17 (s, 3H), 1.08–1.05 (m, 1H), 1.00 (s, 3H), 0.99–0.96 (m, 2H), 0.94 (d, 6H), 0.88 (d, 6H), 0.79 (s, 3H), 0.77–0.72 (m, 1H).  $^{13}\text{C}$  NMR (151 MHz,  $\text{CDCl}_3$ )  $\delta$  144.21, 122.37, 79.00, 69.71, 55.16, 47.57, 46.46, 42.34, 41.72, 39.78, 38.78, 38.59, 36.94, 36.93, 34.08, 33.20, 32.57, 31.03, 30.96, 28.09, 27.22, 25.95, 25.55, 23.58, 23.53, 22.00, 18.35, 16.73, 15.58, 15.52. LC/MS (ESI): Calcd. for  $\text{C}_{30}\text{H}_{51}\text{O}_2^+$  ( $[\text{M}+\text{H}]^+$ ) 443.3, Found. 443.3.

Compound **38**, white solid,  $^1\text{H}$  NMR (600 MHz, DMSO)  $\delta$  6.77 (d,  $J=12.1$  Hz, 2H), 5.21 (s, 1H), 4.28 (d,  $J=5.1$  Hz, 1H), 3.01–2.98 (m, 1H), 2.73 (dd,  $J=13.3$ , 3.6 Hz, 1H), 1.88 (td,  $J=13.5$ , 3.3 Hz, 1H), 1.80 (dd,  $J=8.6$ , 3.0 Hz, 2H), 1.63 (t,  $J=13.5$  Hz, 2H), 1.57–1.37 (m, 9H), 1.36–1.26 (m, 2H), 1.23–1.21 (m, 1H), 1.11–1.09 (m, 4H), 1.04 (d,  $J=11.4$  Hz, 1H), 0.93–0.91 (m, 1H), 0.87 (q, 12H), 0.72 (s, 3H), 0.68–0.66 (m, 4H).  $^{13}\text{C}$  NMR (151 MHz, DMSO)  $\delta$  179.26, 144.69, 121.75, 77.29, 55.28, 47.58, 46.61, 45.66, 41.74, 40.97, 39.32, 38.85, 38.52, 37.07, 34.13, 33.42, 33.09, 32.92, 30.91, 28.71, 27.49, 27.43, 26.11, 23.99, 23.37, 22.84, 18.49, 17.41, 16.49, 15.58. LC/MS (ESI): Calcd. for  $\text{C}_{30}\text{H}_{50}\text{NO}_2^+$  ( $[\text{M}+\text{H}]^+$ ) 456.4, Found. 456.4.

Compound **39**, light yellow solid,  $^1\text{H}$  NMR (600 MHz,  $\text{CDCl}_3$ )  $\delta$  6.35 (s, 1H), 5.95 (s, 1H), 5.34 (t,  $J=3.5$  Hz, 1H), 2.88–2.83 (m, 1H), 2.15–2.06 (m, 2H), 2.04–1.97 (m, 2H), 1.92–1.88 (m, 1H), 1.81–1.69 (m, 4H), 1.65–1.60 (m, 4H), 1.54–1.50 (m, 2H), 1.39–1.33 (m, 4H), 1.22 (d, 6H), 1.14 (s, 3H), 1.11 (s, 3H), 0.94 (s, 3H), 0.91 (s, 3H), 0.83 (s, 3H).  $^{13}\text{C}$  NMR (151 MHz,  $\text{CDCl}_3$ )  $\delta$  201.06, 183.33, 143.87, 143.72, 128.19, 122.08, 53.83, 46.58, 45.59, 43.89, 43.03, 41.99, 41.15, 39.98, 38.45, 33.78, 33.05, 32.44, 32.37, 31.59, 30.68, 27.58, 27.18, 26.97, 25.87, 23.54, 23.38, 22.82, 22.66, 21.80, 19.67, 18.68, 17.44, 14.12. LC/MS (ESI): Calcd. for  $\text{C}_{30}\text{H}_{43}\text{O}_4^-$  ( $[\text{M}-\text{H}]^-$ ) 467.3, Found. 467.3.

Compound **40**, white solid,  $^1\text{H}$  NMR (600 MHz, DMSO)  $\delta$  11.95 (s, 1H), 5.16 (t,  $J=3.3$  Hz, 1H), 2.55–2.45 (m, 1H), 2.32–2.88 (m, 1H), 2.12 (d,  $J=11.3$  Hz, 1H), 1.96–1.89 (m, 3H), 1.85–1.73 (m, 2H), 1.64–1.36 (m, 9H), 1.36–1.22 (m, 4H), 1.06 (s, 3H), 1.04–1.02 (m, 1H), 1.00–0.92 (q, 12H), 0.85–0.76 (d, 6H).  $^{13}\text{C}$  NMR (151 MHz, DMSO)  $\delta$  216.70, 178.75, 138.71, 124.95, 54.68, 52.93, 47.36, 47.06, 46.49, 42.26, 38.96, 36.77, 36.64, 34.16, 32.57, 30.66, 28.02, 26.84, 24.28, 23.64, 23.46, 21.62, 21.52, 19.60, 17.49, 17.28, 15.31. LC/MS (ESI): Calcd. for  $\text{C}_{30}\text{H}_{45}\text{O}_3^-$  ( $[\text{M}-\text{H}]^-$ ) 453.3, Found. 453.3.

Compound **41**, white solid,  $^1\text{H}$  NMR (600 MHz, DMSO)  $\delta$  11.95 (s, 1H), 5.14 (t,  $J=3.4$  Hz, 1H), 4.43–4.40 (m, 1H), 2.12 (d,  $J=11.3$  Hz, 1H), 2.01 (s, 3H), 1.98–1.92 (m, 1H), 1.91–1.77 (m, 3H), 1.67–1.41 (m, 10H), 1.39–1.22 (m, 4H), 1.07 (s, 3H), 1.04–1.00 (m, 3H), 0.92 (d, 6H), 0.86–0.84 (m, 1H), 0.85–0.80 (m, 9H), 0.77 (s, 3H).  $^{13}\text{C}$  NMR (151 MHz, DMSO)  $\delta$  178.75, 170.58, 138.71, 124.91, 80.37, 54.97, 52.83, 47.29, 47.24, 42.13, 38.96, 38.88, 38.17, 37.72, 36.89, 36.78, 32.97, 30.64, 28.27, 28.00, 24.26, 23.70, 23.29, 21.54, 21.45, 18.24, 17.52, 17.35, 17.16, 15.63. LC/MS (ESI): Calcd. for  $\text{C}_{32}\text{H}_{49}\text{O}_4^-$  ( $[\text{M}-\text{H}]^-$ ) 497.3, Found. 497.3.

Compound **42**, white solid,  $^1\text{H}$  NMR (600 MHz, DMSO)  $\delta$  12.14 (ds, 3H), 5.13 (s, 1H), 4.41 (dd,  $J=11.5$ , 4.4 Hz, 1H), 2.48–2.41 (m, 4H), 2.11 (d,  $J=11.4$  Hz, 1H), 1.94–1.80 (m, 4H), 1.66–1.38 (m, 11H), 1.37–1.21 (m, 5H), 1.05 (s, 3H), 1.02–1.96 (m, 2H), 0.91 (d, 6H), 0.82 (d, 9H), 0.76 (s, 3H).  $^{13}\text{C}$  NMR (151 MHz, DMSO)  $\delta$  178.75, 174.12, 173.87, 172.09, 138.71, 124.91, 80.47, 54.99, 52.83, 47.29, 47.22, 38.96, 38.88, 38.12, 37.80, 36.88, 36.78, 32.96, 30.63, 29.64, 29.42, 29.25, 28.21, 28.01, 24.26, 23.71, 23.65, 23.30, 21.54, 18.22, 17.51, 17.35, 17.14, 15.61. LC/MS (ESI): Calcd. for  $\text{C}_{32}\text{H}_{51}\text{O}_6^-$  ( $[\text{M}-\text{H}]^-$ ) 555.3, Found. 555.3.

Compound **43**, light yellow solid.  $^1\text{H}$  NMR (600 MHz,  $\text{CDCl}_3$ )  $\delta$  6.37 (s, 1H), 5.94 (s, 1H), 5.31 (t,  $J=3.4$  Hz, 1H), 2.22 (d,  $J=11.3$  Hz, 1H), 2.19–2.12 (m, 1H), 2.10–2.05 (m, 1H), 2.04–1.99 (m, 1H),

1.91–1.83 (m, 2H), 1.76–1.66 (m, 4H), 1.63–1.48 (m, 6H), 1.42–1.39(m, 1H), 1.36–1.29 (m, 3H), 1.24 (s, 3H), 1.22 (s, 3H), 1.11 (s, 3H), 1.09 (s, 3H), 0.96–0.95 (m, 3H), 0.87 (s, 3H), 0.85 (s, 3H).  $^{13}\text{C}$  NMR (151 MHz,  $\text{CDCl}_3$ )  $\delta$  201.08, 183.29, 143.73, 138.40, 128.34, 125.20, 53.85, 52.66, 48.02, 43.89, 42.94, 42.38, 40.17, 38.92, 38.79, 38.31, 36.62, 32.76, 30.57, 27.90, 27.23, 26.92, 23.99, 23.51, 23.30, 21.78, 21.13, 19.77, 18.67, 17.51, 16.94. LC/MS (ESI): Calcd. for  $\text{C}_{30}\text{H}_{43}\text{O}_4^-$  ( $[\text{M}-\text{H}]^-$ ) 467.3, Found. 467.3.

### 2.3. Fluorescence-based enzyme inhibition assays

#### 2.3.1. Inhibition of triterpenoids on PL-mediated 4-MUO hydrolysis

4-MUO was used as a fluorescent probe substrate to detect the inhibitory effect of triterpenoids on PL in a black standard 96-well plate, while DMSO and orlistat were used as negative and positive controls, respectively. In addition, the background fluorescence in the absence of an enzyme source (PL) (add the same amount of citrate- $\text{Na}_2\text{HPO}_4$  buffer) was measured. The detailed method has been reported in our previous articles<sup>46,47</sup>, the total volume of the incubation mixture was 200  $\mu\text{L}$ , in short, the compound and PL enzyme source were placed in 0.1 M citrate- $\text{Na}_2\text{HPO}_4$  buffer and pre-incubated at 37 °C for 3 min. Then start the reaction by adding 2  $\mu\text{L}$  of 4-MUO probe (3  $\mu\text{M}$ , final concentration). The fluorescence signal of 4-MU (hydrolytic metabolite) was detected by multi-mode microplate reader (SpectraMax M4, Molecular Devices, Urstein, Austria) with continuous oscillation for 20 min and recorded and analysed at 60 s intervals. The excitation wavelength and emission wavelength of 4-MU were set at 340 nm and 460 nm, respectively, and the gain value was 500. The inhibitors are all prepared with DMSO, the final DMSO concentration was 1% (v/v, does not affect the catalytic activity), and the remaining activity was calculated according to the following formula: residual activity (%) = (inhibitor-hydrolysate fluorescence intensity under background fluorescence)/(the hydrolysate fluorescence intensity of the background fluorescence of the negative control (DMSO only)  $\times$  100%.

#### 2.3.2. Inhibition of triterpenoids on hCES1A-mediated NLMe hydrolysis

*N*-Alkylated  $\text{D}$ -luciferin methyl ester (NLMe), a Specific probe for hCES1A<sup>45</sup>, was used for assessing the inhibitory effects for triterpenoids, and BNPP was used as a positive inhibitor of hCES1A. The system for the determination of hCES1A was as follows: first, each compound (2  $\mu\text{L}$ ) and HLM (5  $\mu\text{L}$ , 0.02 mg/mL, initial concentration) were incubated in PBS (91  $\mu\text{L}$ , pH 6.5) for 3 min at 37 °C. Then NLMe (2  $\mu\text{L}$ , 0.15 mM) was added to start the reaction. After shaking the reaction in 37 °C incubator for 10 min, 50  $\mu\text{L}$  of reaction solution was removed and mixed with LDR (50  $\mu\text{L}$ ) to terminate the reaction. A multi-mode microplate reader was used to detect the luminescence signal of NL (the hydrolysed metabolite of NLMe). The luminescence product of NL was measured at 580 nm (gain: 140). The final volume ratio of DMSO was less than 1% (V/V).

#### 2.3.3. Inhibition of triterpenoids on hCES2A-mediated FD hydrolysis

Fluorescent diacetate (FD) was used as the hCES2A specific probe substrate to assay the inhibitory effect of natural triterpenoids on hCES2A. The entire detailed operation process refers to the previously reported method<sup>32</sup>, and finally the FD mixture was put into the multi-mode microplate reader for analysis and detection. The excitation wavelength of the hydrolysed metabolites of FD was 480 nm and the emission wavelength was 525 nm.

#### 2.3.4. Inhibition of triterpenoids on DPP-IV-mediated GP-BAN hydrolysis

Glycyl-prolyl-*N*-butyl-4-amino-1,8-naphthalimide (GP-BAN) was used as a substrate to evaluate the inhibitory effects of triterpenoids against dipeptidyl peptidase-IV (DPP-IV)<sup>48</sup>. The details for DPP-IV inhibition has been reported previously<sup>49,50</sup>. The fluorescent signal of the hydrolytic product (BAN) was measured by a fluorescence microplate reader at an excitation wavelength of 430 nm, an emission wavelength of 535 nm (gain = 500).

#### 2.3.5. Inhibition of triterpenoids on BuChE-mediated BTCH hydrolysis

To assay the inhibitory effects of triterpenoids on Butyrylcholinesterase (BuChE), butyrylthiocholine (BTCH) was used as a substrate for BuChE, The total volume of the system was 100  $\mu\text{L}$ . Including 2  $\mu\text{L}$  DMSO/inhibitor, 2  $\mu\text{L}$  human serum, 84  $\mu\text{L}$  buffered PBS (pH 7.4, 0.1 M), 10  $\mu\text{L}$  substrate iodised butyrylthiocholine (0.3 mM, final concentration) and 2  $\mu\text{L}$  developer 5–5'-dithiobis(2-nitrobenzoic acid) (DTNB) (1 mM, final concentration). The assay protocol of trypsin inhibition was depicted previously<sup>32</sup>. All measurements were performed in triplicates.

### 2.4. Inhibition kinetic analysis

The  $\text{IC}_{50}$  (the concentration of the inhibitor that reduces the enzyme activity by 50%) of the compound with strong inhibitory ability (compound **39/41**) against PL and hCES1A was assayed, using the above inhibitor detection conditions. Subsequently, various concentrations of substrates (selected according to  $K_m$ ) and different concentrations of inhibitors were used to determine the corresponding reaction rate, and the second slope graph of the Lineweaver–Burk diagram was used as a function of the inhibitor to calculate the corresponding inhibition constant ( $K_i$ ) value. All kinetic data were fitted by the following kinetic equations (a–c), for competitive (a), non-competitive (b) and mixed inhibition (c):

$$V = (V_{\max}S)/[K_m(1 + I/K_i) + S] \quad (\text{a})$$

$$V = (V_{\max}S)/[(K_m + S) \times (1 + I/K_i)] \quad (\text{b})$$

$$V = (V_{\max}S)/[(K_m + S) \times (1 + I/\alpha K_i)] \quad (\text{c})$$

where  $V$  is the hydrolytic velocity of the reaction,  $V_{\max}$  is the maximum velocity.  $S$  and  $I$  are substrate (4-MUO, NLMe) and inhibitor (compound **39/41**) concentrations, respectively.  $K_i$  is the inhibition constant of the tested inhibitor against the target PL and hCES1A;  $K_m$  is the Michaelis constant (the substrate concentration at half of the  $V_{\max}$ ).

### 2.5. Statistical analysis

All measurements were made in triplicate and the data obtained in the experiment were shown as mean  $\pm$  SD. The  $\text{IC}_{50}$  and  $K_i$  values of the compounds with strong inhibitory effect were evaluated by nonlinear regression with graphpad prism 7.0 software (GraphPad Software, Inc., La Jolla, CA).

### 2.6. Molecular docking

To explore the binding mechanisms of compounds **39** and **41** against two proteins at the molecular level, the structures of PL (PDB: 1ETH) and hCES1A (PDB: 1MX5) were download from <https://www.rcsb.org/> as receptors and compounds **39** and **41** as ligand, molecular docking was performed with AutoDock Vina (Version 1.1.2) based on Lamarckian genetic algorithm<sup>51</sup>.

Hydrogen atoms were added followed by assigning the Kollman charges. The centre of grid box was set to  $60 \times 60 \times 60 \text{ \AA}^3$  with the spacing of 0.375, enclosing the known binding sites reported previously<sup>52,53</sup>, i.e. the Ser221 of hCES1A and the Ser153 for active site (Site I) and the surface between lipase and colipase for interface site of PL (Site II). Favourable binding processes with the lowest binding energy were indicated for the follow-up calculation.

### 2.7. Cytotoxicity assays

The effect of compounds **39** and **41** on cell viability of the 3T3-L1 cells was measured using Cell Counting Kit-8 (Dalian Meilun Biotechnology Co., Ltd., Dalian, China). Briefly, 3T3-L1 cells ( $5 \times 10^4/\text{mL}$ ,  $100 \mu\text{L}$ ) were seeded in the 96-well plate. After 24 h incubation, then the cells were treated with different concentrations of compounds **39** and **41** (0– $100 \mu\text{M}$ ) for another 48 h. Then, CCK-8 (10%, v/v,  $100 \mu\text{L}$ ) was added to each well and incubated at  $37^\circ\text{C}$  for additional 2 h. The absorbance was determined by microplate reader at 450 nm. The percentage of cell viability was calculated towards control. Each condition included replicate wells with at least four independent repeats.

### 2.8. Cell culture

3T3-L1 cells (ATCC CL-173, Manassas, VA) were cultured in Meilunbio Dulbecco's Modified Eagle Medium/F:12 (DMEM/F:12), supplemented with 10% FBS, and 1% penicillin–streptomycin at  $37^\circ\text{C}$  with 5%  $\text{CO}_2$ . The method of 3T3-L1 cell differentiation into adipocytes refers to our previous article<sup>54</sup>. The cells were planted in a well plate and cultured for 48 h after the cells were 100% confluent. Mix inhibitors compounds **39** and **41** with solution I ( $10 \mu\text{g}/\text{mL}$  insulin in DMEM/F: 12 medium, 0.5 mM 3-isobutyl-1-methylxanthine and 1 mM dexamethasone) to different concentrations, then added to different wells and incubated for 48 h, then the inhibitor was mixed with solution II ( $5 \mu\text{g}/\text{mL}$  insulin in DMEM/F: 12 medium), then added to the wells of the same concentration and incubated for 48 h. Then, the medium in the well was replaced with DMEM/F:12 medium with different concentrations of inhibitors, and the culture was continued for 48 h.

### 2.9. Oil red O staining

The lipid droplets of 3T3-L1 cells were stained with Oil Red O stain kit (Beijing solebo Technology Co., Ltd., Beijing, China) after cultured for 48 h. In short, 3T3-L1 cells were washed with PBS 2 times and fixed with ORO fixative for 20–30 min, and then washed again with deionised water for 3 times. Then, 3T3-L1 cells were washed with 60% isopropanol for 5 min, immersed in oil red O solution for 10–20 min, and washed with deionised water for 3–5 times. Mayer's haematoxylin staining solution was added, the nucleus was stained for 1–2 min, then washed for 3–5 times, and Oro buffer solution was added for 1 min. Finally, distilled water was added to cover the cells. The stained lipid droplets were observed under inverted microscope (Lecai DMI8).

## 3. Results and discussion

### 3.1. Screening of PL inhibitors from natural triterpenoids

In this study, the inhibitory effects of 27 natural triterpenoids (Scheme 1) against PL were determined. As shown in Table 1, oleanolic acid (**1**) and ursolic acid (**5**) were found to display good inhibitory effects on PL, while natural pentacyclic triterpenoids

(**2–4**, **6**, **7**) with more hydroxyl group compared to oleanolic acid (**1**) and ursolic acid (**5**), displayed less potency towards PL.  $\beta$ -Boswellic acid (**8**) with carboxyl group at the C-23 site displayed potent inhibitory effects against PL, while glycyrrhetic acid (**9**) with carboxyl group at the C-30 site exhibited less inhibitory effects. Furthermore, glycyrrhizic acid (**10**) with the glycosidic group at the C-3 site demonstrated poor inhibitory effects on PL. Structure–activity relationships (SAR) analysis suggested that natural pentacyclic triterpenoids with more hydroxyl group and glycosidic group may be not beneficial for PL inhibition. Celastrol (**11**) and betulin (**12**) showed good inhibitory effects on PL, while betulin homologues (**13–15**) displayed a decrease of inhibitory effects on PL. In addition, pachymic acid (**16**), ganoderic acid B (**17**) and ginsenosides (**18–27**) exhibited less potent or poor inhibitory effects on PL, which suggested that the long alkyl chain at the C-20 site of triterpenoids and glycosidic group could be unbeneficial for PL inhibition.

### 3.2. Inhibitory effects of natural triterpenoids against hCES1A and hCES2A

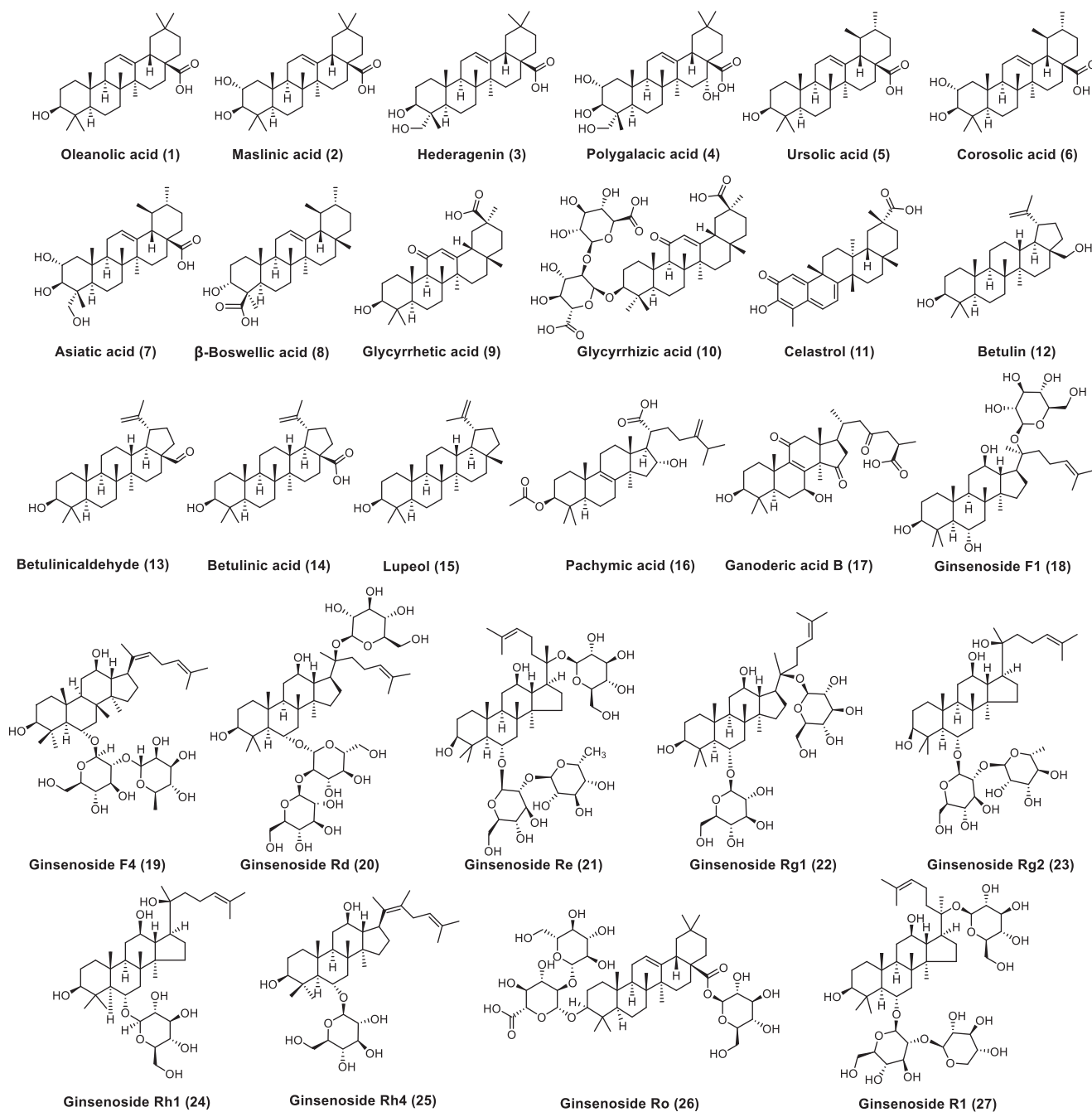
Above studies shown that there were nine natural triterpenoids with moderate inhibitory effect against PL ( $\text{IC}_{50} < 20 \mu\text{M}$ ). Thus, a further investigation was carried out to evaluate the inhibitory effects of these compounds on hCES1A and hCES2A using NLMe and FD as specific optical substrate, respectively. As shown in Table 2, except for  $\beta$ -boswellic acid (**8**) and betulin (**12**), other seven triterpenoids showed moderate to strong inhibitory effect on the hydrolysis of hCES1A-mediated NLMe. It was found from these natural triterpenoids that the OA (**1**) and UA (**5**) have the good inhibitory effects against hCES1A and PL, and highly selectivity over hCES2A. These results encouraged us to design and synthesise a batch of compounds based on the scaffolds of OA and UA to obtain potent dual target inhibitors of hCES1A and PL.

### 3.3. Synthesis of OA and UA derivatives

Compounds **31–43** were synthesised according to Scheme 2. Compounds **30** and **40** were obtained in high yield from OA (**1**) and UA (**5**) with the Jones' reagent, respectively. OA (**1**) and UA (**5**) were introduced acetyl in C-3 with acetic anhydride in pyridine to obtain compounds **31** and **41** with high yield (88–92%), respectively. Compound **31** was then treated with oxalyl chloride, without isolation, further reacted with concentrated ammonia to afford compound **32** in a yield of 64%. The  $3\beta$ -hydroxy group of OA (**1**) and UA (**5**) were reacted with succinic anhydride in the presence of 4-dimethylaminopyridine (DMAP) to obtain the target products **33** and **42**, respectively. OA (**1**) reacted with *n*-butyric anhydride and *n*-hexanoic anhydride to afford compounds **34** and **35**, respectively. Reaction of the iodomethane with OA furnished the target compound **36**. The OA was reduced with lithium aluminium hydride to afford the compound **37**. Compound **32** was hydrolysed under the effectiveness of NaOH to afford compound **38** in 86% yield. OA (**1**) and UA (**5**) were treated with Jones' reagent, and further reacted with *t*-BuOK to afford compounds **39** and **43**, respectively.

### 3.4. Inhibitory effects of OA and UA derivatives against PL and hCES1A

A batch of OA and UA derivatives were synthesised. We further evaluated the inhibitory effects of these fourteen derivatives on



**Scheme 1.** Chemical structure of natural triterpenoids.

PL and hCES1A. As shown in Table 3, the 3-keto-OA derivative (**30**) exhibited similar trends in PL inhibition as OA, while the compound **31** with carbonyl group at the C-3 site resulted in an increase of inhibitory effect on PL compared with OA. Compounds **32** and **38** exhibited relatively low inhibitory activities against PL as compared with compound **31** and OA, respectively, suggesting that the introduction of amides group at C-28 results in a loss of potency. Notably, replacement of the C-3 ethyl ester group with 3-O- $\beta$ -carboxypropionyl, *n*-butyric and *n*-hexanoic in compounds **33–35** led to a dramatically decrease in the inhibitory effects against PL. These results suggested that the structural modifications on the C-3 hydroxyl group of OA with bigger acyl groups such as 3-O- $\beta$ -carboxypropionyl, *n*-butyric and *n*-hexanoic were unbeneficial for the development of potent inhibitors against PL.

Alcohols (**36**) and esters (**37**) derivatives displayed decrease inhibitory effects towards PL compared with OA, while compound **39** with 2-enol and 3-ketal moiety exhibited potent inhibitory effect on PL. Consistently, UA derivatives (**40–43**) exhibited similar trends in PL inhibition as OA derivatives (**30**, **31**, **34** and **39**). Further evaluate the inhibitory effects of fourteen derivatives on hCES1A showed that except for compounds **35** and **37**, other twelve derivatives showed moderate to strong inhibitory effect on the hydrolysis of hCES1A-mediated NLMe.

### 3.5. *Sar* summary of triterpenoids

Based on these results of the inhibitory effects of nature triterpenoids and 14 derivatives on PL and hCES1A, the structure–PL/

**Table 1.** The inhibitory effects of natural triterpenes against PL

Compound	IC <sub>50</sub> (μM) PL	Compound	IC <sub>50</sub> (μM) PL
1	8.63 ± 0.84	15	>100
2	16.02 ± 4.59	16	>100
3	13.01 ± 2.03	17	>100
4	>100	18	>100
5	6.16 ± 0.97	19	74.46 ± 28.42
6	12.79 ± 1.44	20	29.72 ± 5.02
7	12.93 ± 1.87	21	>100
8	0.42 ± 0.05	22	>100
9	28.33 ± 9.47	23	>100
10	>100	24	>100
11	4.69 ± 0.37	25	>100
12	7.47 ± 1.68	26	>100
13	>100	27	>100
14	>100	28	0.2345 ± 0.029

Data were shown as mean ± SD (*n* = 3). 28\* Orlistat, a PL positive inhibitors.

**Table 2.** The inhibitory effects of natural triterpenes against hCES1A, hCES2A and PL

Compound	IC <sub>50</sub> (μM) hCES1A	IC <sub>50</sub> (μM) hCES2A	IC <sub>50</sub> (μM) PL
1	0.04 ± 0.003	6.02 ± 0.54	8.63 ± 0.84
2	0.12 ± 0.01	5.91 ± 1.65	16.02 ± 4.59
3	0.04 ± 0.004	9.22 ± 1.43	13.01 ± 2.03
5	0.04 ± 0.004	7.38 ± 1.10	6.16 ± 0.97
6	0.34 ± 0.04	14.45 ± 2.01	12.79 ± 1.44
7	0.17 ± 0.02	65.08 ± 6.41	12.93 ± 1.87
8	>100	/	0.42 ± 0.05
11	14.27 ± 3.03	2.31 ± 0.12	4.69 ± 0.37
12	>100	/	7.47 ± 1.68
28	0.035 ± 0.003	1.83 ± 0.26 (nM)	0.23 ± 0.03
29	0.36 ± 0.03	3.08 ± 0.77	>100

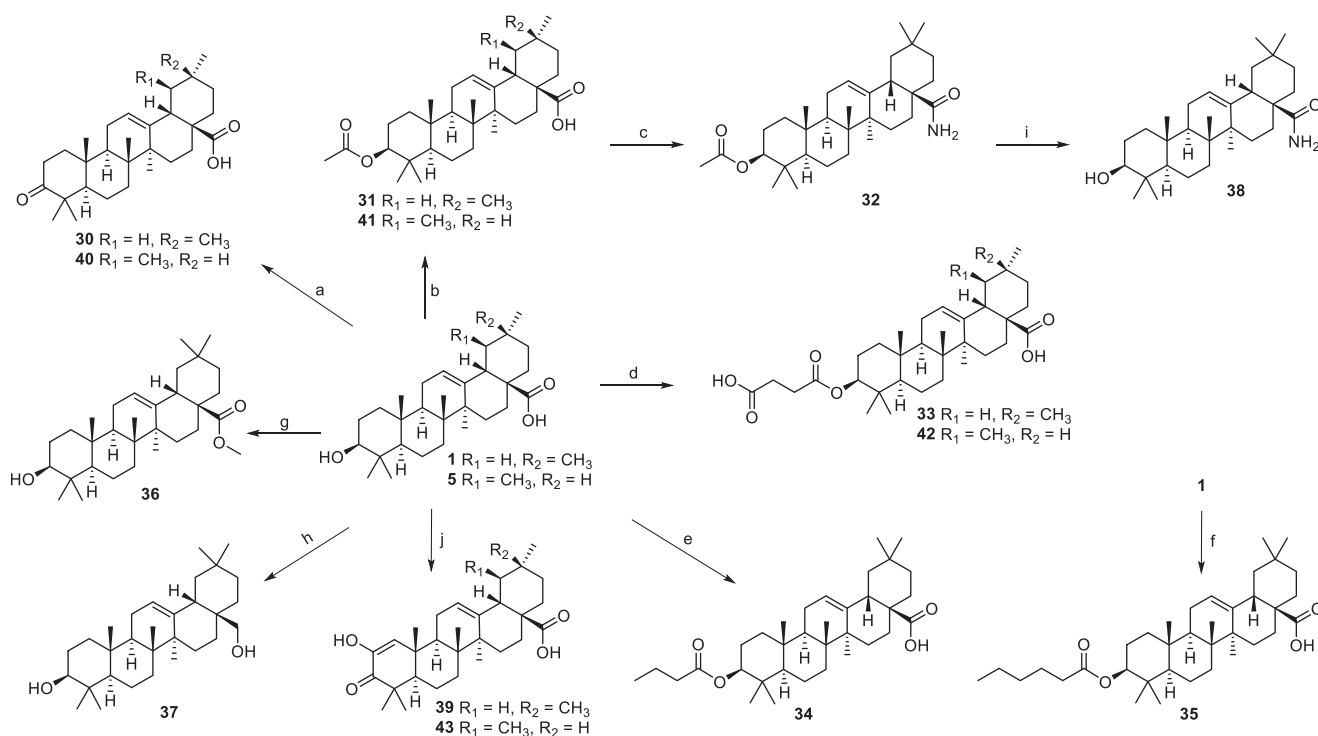
Data were shown as mean ± SD (*n* = 3). 28\* Orlistat, a PL positive inhibitor. 29\* BNPP, broad-spectrum inhibitor of hCES1A and hCES2A.

hCES1A inhibition relationships of these triterpenoids are summarised as follows, (1) natural pentacyclic triterpenoids with more hydroxyl group and glycosidic group are not beneficial for PL inhibition, (2) triterpenoids with 2- enol and 3-ketal moiety are beneficial for PL and hCES1A inhibition, (3) structural modifications on the C-3 hydroxyl group with bigger acyl groups were unbeneficial for PL inhibition, while replacement of C-3 hydroxyl group with ester led to improved inhibitory effects towards hCES1A, (4) long alkyl chain at the C-20 site of triterpenoids and glycosidic group could be unbeneficial for PL inhibition, (5) carboxyl group at the C-23 site is beneficial for PL inhibition but not good for hCES1A inhibition, while carboxyl group at the C-30 site is unbeneficial for PL inhibition, and (6) replacement of C-28 carboxyl group with ester, amide or alcohol are unbeneficial for both PL and hCES1A inhibition (Figure 1). These key findings are very helpful for pharmacochemists to better understand the SAR of triterpenoids for both PL and hCES1A inhibition and to develop novel dual inhibitors using triterpenoids as leading compounds.

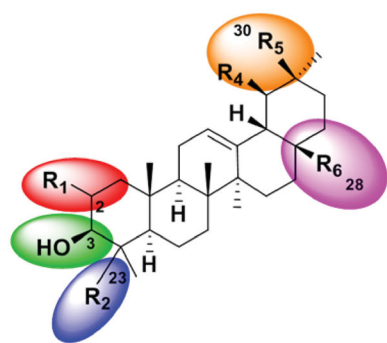
**Table 3.** The inhibitory effects of OA and UA derivatives against PL and hCES1A.

Compound	IC <sub>50</sub> (μM) PL	IC <sub>50</sub> (μM) hCES1A	Compound	IC <sub>50</sub> (μM) PL	IC <sub>50</sub> (μM) hCES1A
30	7.51 ± 1.08	0.047 ± 0.003	37	11.78 ± 1.60	4.106 ± 0.77
31	3.67 ± 0.72	0.051 ± 0.005	38	7.83 ± 1.21	0.48 ± 0.06
32	7.02 ± 0.59	0.11 ± 0.013	39	2.13 ± 0.19	0.055 ± 0.006
33	36.39 ± 5.17	0.043 ± 0.003	40	6.94 ± 1.37	0.93 ± 0.18
34	>100	0.24 ± 0.049	41	0.75 ± 0.12	0.014 ± 0.002
35	>100	1.82 ± 0.29	42	20.87 ± 1.78	0.028 ± 0.003
36	30.59 ± 3.58	0.856 ± 0.15	43	5.21 ± 1.24	0.032 ± 0.003

Data were shown as mean ± SD (*n* = 3).



**Scheme 2.** Synthetic route of OA and UA derivatives. Reagents and conditions: (a) Jones reagent, acetone, 0 °C, 1 h, 72–80%; (b) acetic anhydride, pyridine, rt, 24 h, 88–92%; (c) (COCl)<sub>2</sub>, CH<sub>2</sub>Cl<sub>2</sub>, rt, 2 h, then conc. ammonia, toluene, 4–8 °C, 2 h, 64%; (d) succinic anhydride, DMAP, CH<sub>2</sub>Cl<sub>2</sub>, rt, 24 h, 85–93%; (e) *n*-butyric anhydride, DMAP, CH<sub>2</sub>Cl<sub>2</sub>, rt, 24 h, 64%; (f) *n*-hexanoic anhydride, DMAP, CH<sub>2</sub>Cl<sub>2</sub>, rt, 24 h, 71%; (g) CH<sub>3</sub>I, K<sub>2</sub>CO<sub>3</sub>, acetone, rt, 12 h, 88%; (h) LiAlH<sub>4</sub>, THF, rt, 24 h, 60%; (i) NaOH, MeOH/THF, 40 °C, 5 h, 86%; (j) Jones reagent, acetone, 0 °C, 1 h, then, *t*-BuOK/*t*-BuOH, THF, 31–34%.



- 2-Enol and 3-ketal moiety are beneficial for PL and hCES1A inhibition
- Smaller 3-acetyl group is beneficial for PL inhibition, while bigger 3-O- $\beta$ -carboxypropionyl group is beneficial for hCES1A
- 23-Carboxyl group is beneficial for PL inhibition but not good for hCES1A, while 30-carboxyl group is unbeneficial for PL inhibition
- Replacement of C-28 carboxyl group with ester, amide or alcohol are unbeneficial for both PL and hCES1A inhibition

Figure 1. SAR summary of triterpenoids.

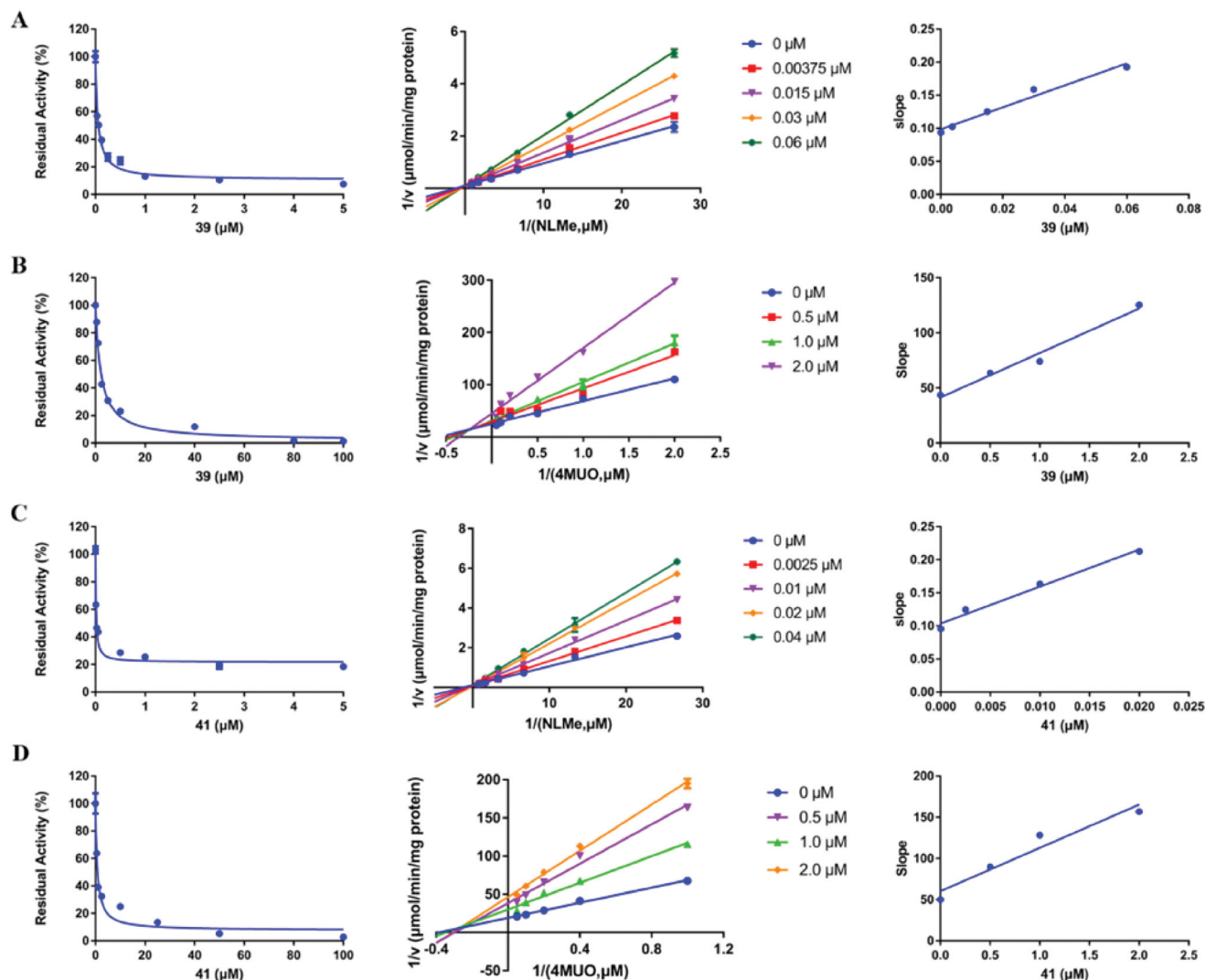


Figure 2. (A) Inhibition behaviours of **39** against hCES1A-mediated NLMe hydrolysis. (B) Inhibition behaviours of **39** against PL mediated 4-MUO hydrolysis. (C) Inhibition behaviours of **41** against hCES1A-mediated NLMe hydrolysis. (D) Inhibition behaviours of **41** against PL mediated 4-MUO hydrolysis. *Left*: the dose-dependent inhibition curve. *Middle*: the Lineweaver–Burk plot. *Right*: the second plot of slopes from the Lineweaver–Burk plots. All data represent the mean of triplicate determinations.

### 3.6. Inhibition kinetic analyses

In order to explore the inhibitory mechanism of two dual-target potent inhibitors (**39** and **41**) on PL and hCES1A, inhibitory kinetic analysis was carried out. As shown in Figures S1 and S2, the dose-response curves of compounds **39** and **41** were not affected by the pre-incubation times, indicating that compounds **39** and **41** were reversible inhibitors against PL and hCES1A. Then, the

inhibitory kinetics of compounds **39** and **41** against hCES1A were characterised in HLM. As shown in Figure 2(A,C), the results clearly show that both **39** and **41** inhibit the hCES1A-mediated hydrolysis of NLMe in HLM in a competitive manner, and the inhibition constants ( $K_i$ ) of **39** and **41** were calculated 0.043  $\mu\text{M}$  and 0.019  $\mu\text{M}$ , respectively. In addition, the inhibitory kinetics of compounds **39** and **41** against PL were characterised in PL. As shown in

Figure 2(B,D), both **39** and **41** inhibited PL-mediated 4-MUO hydrolysis through a mixed manner, and the inhibition constants ( $K_i$ ) of **39** and **41** were calculated 1.45  $\mu\text{M}$  and 0.58  $\mu\text{M}$ , respectively.

### 3.7. Specificity of **39** and **41** towards hCES1A and PL over other human serine hydrolases

In view of the overlap of mammalian serine hydrolases, it is necessary to study the specificity of **39** and **41** on hCES1A and PL over other human serine hydrolases. In this study, three other human serine hydrolases (hCES2A, DPP-IV and BuChE) were used to study the specificity of the dual-target inhibitors. As shown in Table 4, both compounds **39** and **41** were found with good selectivity over hCES2A and high selectivity over BuChE and DPP-

IV. These indicate that compounds **39** and **41** are selective inhibitors of hCES1A and PL.

### 3.8. Docking simulation

In order to gain insight into the interaction mode between inhibitors (compounds **39** and **41**) and targets (PL and hCES1A), molecular docking simulations were carried out, respectively. The binding modes between compound **39/41** and hCES1A were explored firstly. As shown in Figure 3 and Table S1, both **39** and **41** could be well docked into the catalytic cavity of hCES1A. Compared to original ligand homotropine in crystal structure (PL, PDB: 1ETH; hCES1A, PDB: 1MX5), they occupy the position of homotropine, and could block the active site more completely, and the predicted binding energy were  $-9.4\text{ kcal/mol}$  and  $-9.6\text{ kcal/mol}$ , respectively. The detailed interaction (Figure S3) shows that their main mode of action was hydrophobic interaction. In addition, the binding poses between compound **39/41** and PL were explored as shown in Figure 3 and Table S1. At Site I (the Ser-153 for active site), hydrophobic interaction was the main interaction, and the energy were  $-7.4\text{ kcal/mol}$  and  $-7.5\text{ kcal/mol}$ , respectively. Both compounds **39/41** and ethylene glycol mono-octyl ether (TGME), the original ligand of crystal structure, have hydrophilic and hydrophobic groups at both ends. The carboxyl in **39/41** tend to point to the solvent and occupy around the pocket to affect substrate entry. In addition, at Site II (the surface between lipase and colipase for interface site of PL), compound **38** can form hydrogen bond with Arg-65, and compound **41** can interact with Arg-65 and Lys-42 through hydrogen bonds (Figure S4), with energies of  $-8.6\text{ kcal/mol}$  and  $-8.6\text{ kcal/mol}$ , respectively.

Table 4. The inhibitory effects of **39** and **41** towards five serine hydrolases.

Compound	Target enzyme	Substrate	IC <sub>50</sub> ( $\mu\text{M}$ )	K <sub>i</sub> ( $\mu\text{M}$ )	Inhibition mode
<b>39</b>	PL	4-MUO	2.13 $\pm$ 0.19	1.45	Mixed
	hCES1A	NLMe	0.055 $\pm$ 0.006	0.059	Competitive
	hCES2A	FD	6.02 $\pm$ 0.75	–	–
	BuChE	GP-BAN	>100	–	–
	DPP-IV	BTCH	>100	–	–
<b>41</b>	PL	4-MUO	0.75 $\pm$ 0.12	0.58	Mixed
	hCES1A	NLMe	0.014 $\pm$ 0.002	0.019	Competitive
	hCES2A	FD	5.02 $\pm$ 0.88	–	–
	BuChE	GP-BAN	>100	–	–
	DPP-IV	BTCH	>100	–	–

Data were shown as mean  $\pm$  SD ( $n = 3$ ).

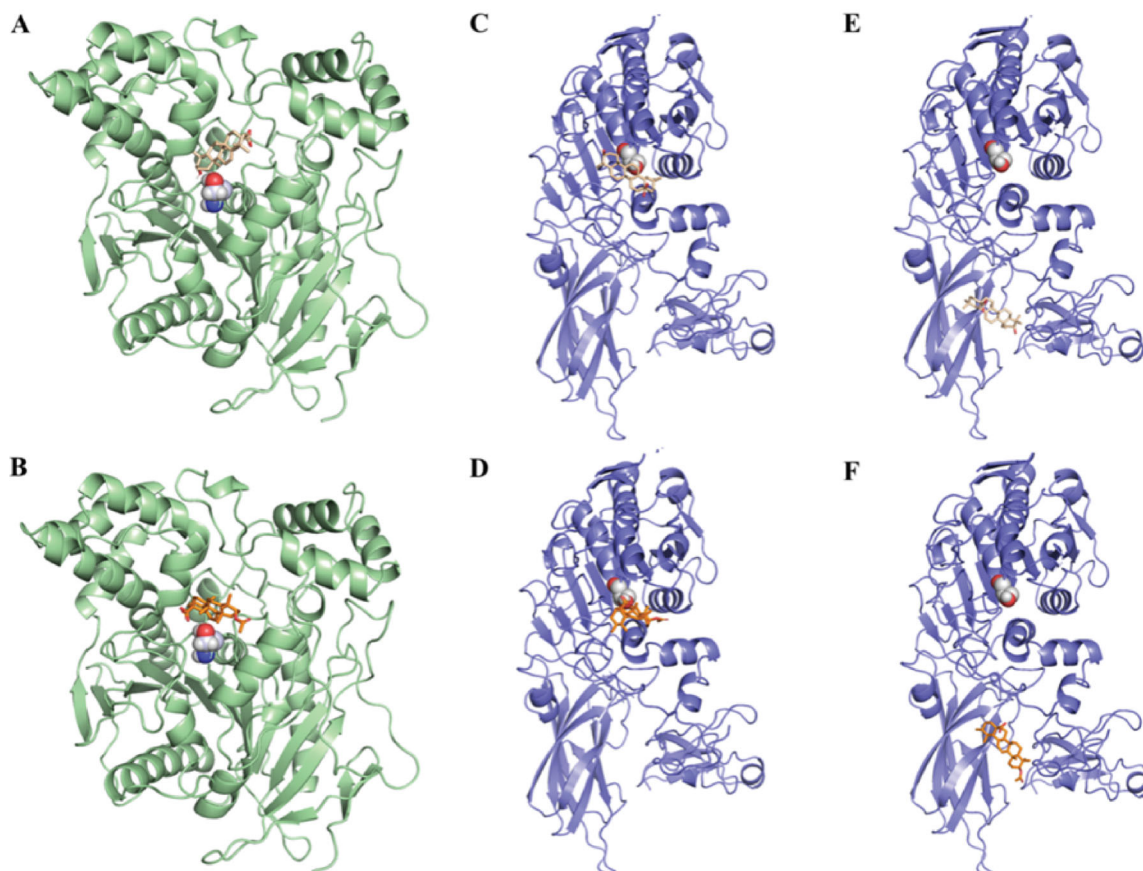
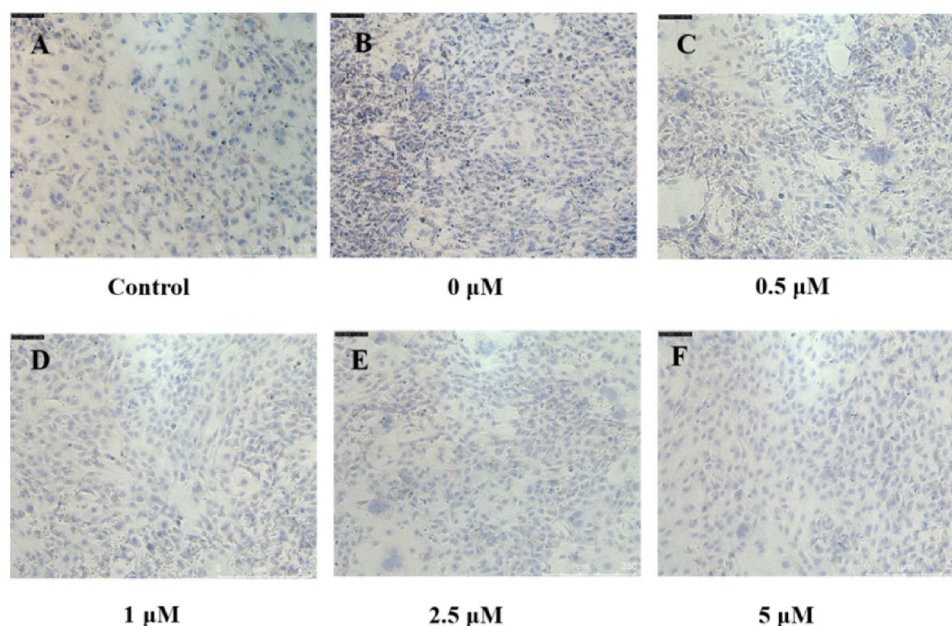
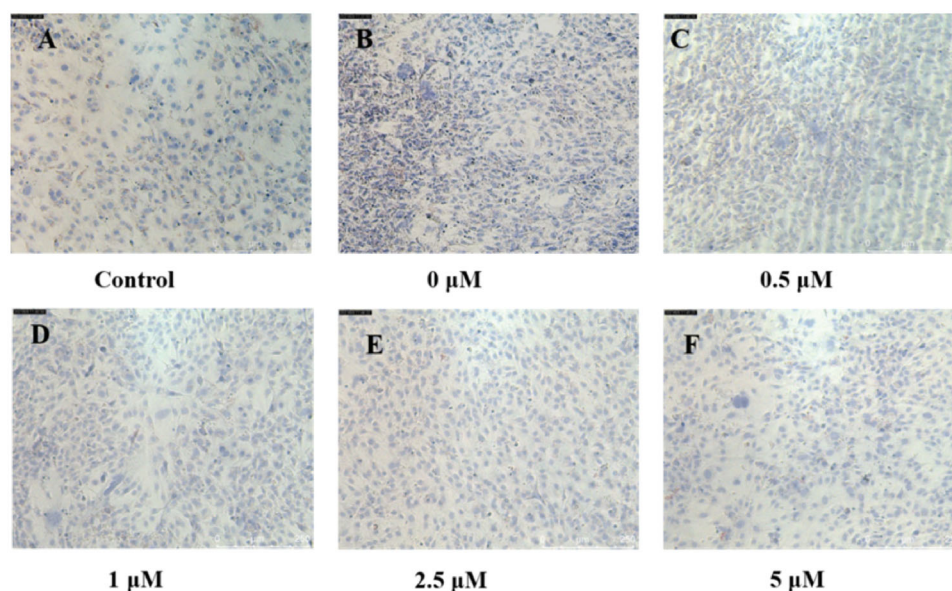


Figure 3. Overview of compounds **39** (A) and **41** (B) docked into the activity pocket of hCES1A. The stereo view of PL docked with compound **39** at site I (C) and site II (D); The stereo view of PL docked with compound **41** at site I (E) and site II (F).



**Figure 4.** Oil red O staining results of 3T3-L1 cells (A) normally cultured and (B–F) differentiation culture treated with compound **39** (0–5  $\mu\text{M}$ ) (magnification, 10 $\times$ ).



**Figure 5.** Oil red O staining results of 3T3-L1 cells (A) normally cultured and (B–F) differentiation culture treated with compound **41** (0–5  $\mu\text{M}$ ) (magnification, 10 $\times$ ).

Colipase interacts with the lipase C-terminal domain (C domain) and with the flap (a surface loop from the N-terminal domain), so we speculated that binding at site II may affect flap movement and thus substrate binding.

### 3.9. Inhibit the formation of lipid droplets in 3T3-L1 cells

In order to study the effects of dual-target inhibitors compounds **39** and **41** on the formation of lipid droplets during the induction of 3T3-L1 mouse preadipocytes into adipocytes, compounds **39** and **41** were added for pre-treatment before cell induction. First, the cell viability test results show that compounds **39** and **41** are almost non-toxic to 3T3-L1 below 20  $\mu\text{M}$  and 10  $\mu\text{M}$ , respectively (Figure S5). Next, compounds **39** and **41** at different concentrations were mixed with an inducer that induces adipocyte

differentiation, and incubated with the cells for 96 h. After culturing with compounds **39** and **41** in normal medium for 96 h, the medium was changed every 2 days, and then the cells were stained with Oil Red O dye. The results showed that the lipid droplets in the induced 3T3-L1 cells (Figure 4(B)) were significantly higher than those in the uninduced control group (Figure 4(A)). In addition, almost no lipid droplets were formed in the cells treated with the high concentration (5  $\mu\text{M}$ ) of compounds **39** and **41** (Figures 4(F) and 5(F)). The formation of lipid droplets in cells treated with low concentrations (<1  $\mu\text{M}$ ) were similar to that of uninduced controls. In addition, it can be seen from Figures 4 and 5(C–F) that the lipid droplet content of compounds **39/41** gradually decreases from low concentration to high concentration. The results indicate that two dual-target inhibitors could inhibit the formation of lipid droplets in adipocytes induced by preadipocytes.

#### 4. Conclusion

In summary, a series of natural triterpenoids were collected and their inhibitory effects against PL and hCES1A were assayed using 4-MUO and NLMe as substrate probe, respectively. Two natural pentacyclic triterpenoid OA and UA were found to display both good inhibitory effects on PL and hCES1A, and good selectivity over hCES2A. Thus, 14 compounds based on the UA and OA skeletons were synthesised and evaluated. Structure-activity relationship (SAR) analysis of these compounds revealed that 2-enol and 3-ketal moiety are beneficial for PL and hCES1A inhibition, and smaller 3-acetyl group is beneficial for PL inhibition, while bigger 3-O- $\beta$ -carboxypropionyl group is beneficial for hCES1A. In addition, compounds **39** (OA derivative with 2-enol and 3-ketal moiety) and **41** (OA derivative with acetyl group at the C-3 site) displayed potent inhibitory effects against both PL and hCES1A. Furthermore, compounds **39** and **41** exhibited good selectivity over other human serine hydrolases including hCES2A, BChE and DPP-IV. Inhibitory kinetics and molecular docking studies demonstrated that both compounds **39** and **41** were effective mixed inhibitors of PL, while competitive inhibitors of hCES1A. Further investigations demonstrated that both compounds **39** and **41** could inhibit adipocyte adipogenesis induced by mouse preadipocytes. Collectively, our findings suggest that triterpenoids are good choices for design and development of PL and hCES1A inhibitors, while compounds **39** and **41** hold great promise for development of novel PL and hCES1A dual-target inhibitors to treat with related metabolic diseases.

#### Disclosure statement

The authors declare that they have no known competing financial interests or personal relationships that could have appeared to influence the work reported in this paper.

#### Funding

Authors are grateful to the NSF of China (81973393), the National Science and Technology Major Project of China (2018ZX09731016), the National Key Research and Development Program of China (2017YFC1702000), and the Special Project of Postgraduate Innovation Training of Shanghai University of Traditional Chinese Medicine (Y2020068).

#### References

- Malik V, Willett W, Hu F. Global obesity: trends, risk factors and policy implications. *Nat Rev Endocrinol* 2013;9:13–27.
- Mameli C, Zuccotti G, Carnovale C, et al. An update on the assessment and management of metabolic syndrome, a growing medical emergency in paediatric populations. *Pharmacol Res* 2017;119:99–117.
- Motamed N, Rabiee B, Roozafai F, et al. Metabolic syndrome and cardiovascular risk assessment tools' estimations of 10-year cardiovascular risk: a population-based study. *Acta Cardiol* 2018;73:439–46.
- Ménégaud L, Thomas C, Lagrost L, Masson D. Fatty acid metabolism in macrophages: a target in cardio-metabolic diseases. *Curr Opin Lipidol* 2017;28:19–26.
- Danaei G, Ding E, Mozaffarian D, et al. The preventable causes of death in the United States: comparative risk assessment of dietary, lifestyle, and metabolic risk factors. *PLoS Med* 2009;6:e1000058.
- Xiao D, Chen Y, Yang D, Yan B. Age-related inducibility of carboxylesterases by the antiepileptic agent phenobarbital and implications in drug metabolism and lipid accumulation. *Biochem Pharmacol* 2012;84:232–9.
- Merali Z, Ross S, Paré G. The pharmacogenetics of carboxylesterases: CES1 and CES2 genetic variants and their clinical effect. *Drug Metab Drug Interact* 2014;29:143–51.
- Hatfield M, Umans R, Hyatt J, et al. Carboxylesterases: general detoxifying enzymes. *Chem-Biol Interact* 2016;259:327–31.
- Wang D, Zou L, Jin Q, et al. Human carboxylesterases: a comprehensive review. *Acta Pharm Sin. B* 2018;8:699–712.
- Lian J, Nelson R, Lehner R. Carboxylesterases in lipid metabolism: from mouse to human. *Protein Cell* 2018;9:178–95.
- Zou L, Jin Q, Wang D, et al. Carboxylesterase inhibitors: an update. *Curr Med Chem* 2018;25:1627–49.
- Ross M, Crow J. Human carboxylesterases and their role in xenobiotic and endobiotic metabolism. *J Biochem Mol Toxicol* 2007;21:187–96.
- Laizure S, Herring V, Hu Z, et al. The role of human carboxylesterases in drug metabolism: have we overlooked their importance? *Pharmacotherapy* 2013;33:210–22.
- Tarkiainen EK, Holmberg MT, Tornio A, et al. Carboxylesterase 1 c.428G>A single nucleotide variation increases the antiplatelet effects of clopidogrel by reducing its hydrolysis in humans. *Clin Pharmacol Ther* 2015;97:650–8.
- Shi D, Yang J, Yang D, et al. Anti-influenza prodrug oseltamivir is activated by carboxylesterase human carboxylesterase 1, and the activation is inhibited by antiplatelet agent clopidogrel. *J Pharmacol Exp Ther* 2006;319:1477–84.
- Zou LW, Li YG, Wang P, et al. Design, synthesis, and structure-activity relationship study of glycyrrhetic acid derivatives as potent and selective inhibitors against human carboxylesterase 2. *Eur J Med Chem* 2016;112:280–8.
- Zou LW, Dou TY, Wang P, et al. Structure-activity relationships of pentacyclic triterpenoids as potent and selective inhibitors against human carboxylesterase 1. *Front Pharmacol* 2017;8:435.
- Dominguez E, Galmozzi A, Chang J, et al. Integrated phenotypic and activity-based profiling links *Ces3* to obesity and diabetes. *Nat Chem Biol* 2014;10:113–21.
- Quiroga A, Li L, Trötzmüller M, et al. Deficiency of carboxylesterase 1/esterase-x results in obesity, hepatic steatosis, and hyperlipidemia. *Hepatology (Baltimore, Md.)* 2012;56:2188–98.
- Wei E, Ben Ali Y, Lyon J, et al. Loss of TGH/*Ces3* in mice decreases blood lipids, improves glucose tolerance, and increases energy expenditure. *Cell Metab* 2010;11:183–93.
- Mukherjee S, Choi M, Yun JW. Novel regulatory roles of carboxylesterase 3 in lipid metabolism and browning in 3T3-L1 white adipocytes. *Appl Physiol Nutr Metab* 2019;44:1089–98.
- Ashla A, Hoshikawa Y, Tsuchiya H, et al. Genetic analysis of expression profile involved in retinoid metabolism in non-alcoholic fatty liver disease. *Hepatol Res* 2010;40:594–604.
- Nagashima S, Yagyu H, Takahashi N, et al. Depot-specific expression of lipolytic genes in human adipose tissues-association among *CES1* expression, triglyceride lipase activity and adiposity. *J Atheroscler Thromb* 2011;18:190–9.
- Gilham D, Ho S, Rasouli M, et al. Inhibitors of hepatic microsomal triacylglycerol hydrolase decrease very low density

- lipoprotein secretion. *FASEB J: Off Publ Federation Am Soc Exp Biol* 2003;17:1685–7.
25. Lian J, Bahitham W, Panigrahi R, et al. Genetic variation in human carboxylesterase CES1 confers resistance to hepatic steatosis. *Biochimica Biophysica Acta. Mol Cell Biol Lipids* 2018;1863:688–99.
  26. Bachovchin DA, Cravatt BF. The pharmacological landscape and therapeutic potential of serine hydrolases. *Nat Rev Drug Discov* 2012;11:52–68.
  27. Birari RB, Bhutani KK. Pancreatic lipase inhibitors from natural sources: unexplored potential. *Drug Discov Today* 2007;12:879–89.
  28. Sukhdev S, Bhupender S, Singh KS. Pharmacotherapy & surgical interventions available for obesity management and importance of pancreatic lipase inhibitory phytochemicals as safer anti-obesity therapeutics. *Mini Rev Med Chem* 2017;17:371–9.
  29. Houghton D, Wilcox MD, Chater PI, et al. Biological activity of alginate and its effect on pancreatic lipase inhibition as a potential treatment for obesity. *Food Hydrocoll* 2015;49:18–24.
  30. de la Garza AL, Milagro FI, Boque N, et al. Natural inhibitors of pancreatic lipase as new players in obesity treatment. *Planta Med* 2011;77:773–85.
  31. Wang DD, Zou LW, Jin Q, et al. Recent progress in the discovery of natural inhibitors against human carboxylesterases. *Fitoterapia* 2017;117:84–95.
  32. Zhao YS, Qian XK, Guan XQ, et al. Discovery of natural alkaloids as potent and selective inhibitors against human carboxylesterase 2. *Bioorg Chem* 2020;105:104367.
  33. Song PF, Zhu YD, Ma HY, et al. Discovery of natural pentacyclic triterpenoids as potent and selective inhibitors against human carboxylesterase 1. *Fitoterapia* 2019;137:104199.
  34. Neovius M, Johansson K, Rössner S. Head-to-head studies evaluating efficacy of pharmacotherapy for obesity: a systematic review and meta-analysis. *Obes Rev* 2008;9:420–7.
  35. Kaila B, Raman M. Obesity: a review of pathogenesis and management strategies. *Can J Gastroenterol* 2008;22:61–8.
  36. Chauhan D, George G, Sridhar SNC, et al. Design, synthesis, biological evaluation, and molecular modeling studies of rhodanine derivatives as pancreatic lipase inhibitors. *Arch Pharm* 2019;352:e1900029.
  37. Hodon J, Borkova L, Pokorny J, et al. Design and synthesis of pentacyclic triterpene conjugates and their use in medicinal research. *Eur J Med Chem* 2019;182:111653.
  38. Hill RA, Connolly JD. Triterpenoids. *Nat Prod Rep* 2017;34:90–122.
  39. Dzubak P, Hajduch M, Vydra D, et al. Pharmacological activities of natural triterpenoids and their therapeutic implications. *Nat Prod Rep* 2006;23:394–411.
  40. Salvador JAR, Leal AS, Valdeira AS, et al. Oleanane-, ursane-, and quinone methide friedelane-type triterpenoid derivatives: recent advances in cancer treatment. *Eur J Med Chem* 2017;142:95–130.
  41. Xiao S, Tian Z, Wang Y, et al. Recent progress in the antiviral activity and mechanism study of pentacyclic triterpenoids and their derivatives. *Med Res Rev* 2018;38:951–76.
  42. Wu P, Zheng J, Huang T, et al. Synthesis and evaluation of novel triterpene analogues of ursolic acid as potential anti-diabetic agent. *PLoS One* 2015;10:e0138767.
  43. Ding YJ, Sun CY, Wen CC, Chen YH. Nephroprotective role of resveratrol and ursolic acid in aristolochic acid intoxicated zebrafish. *Toxins (Basel)* 2015;7:97–109.
  44. Hu Q, Guan XQ, Song LL, et al. Inhibition of pancreatic lipase by environmental xenoestrogens. *Ecotoxicol Environ Saf* 2020;192:110305.
  45. Wang DD, Zou LW, Jin Q, et al. Bioluminescent sensor reveals that carboxylesterase 1A is a novel endoplasmic reticulum-derived serologic indicator for hepatocyte injury. *ACS Sens* 2020;5:1987–95.
  46. Liu PK, Weng ZM, Ge GB, et al. Biflavones from *Ginkgo biloba* as novel pancreatic lipase inhibitors: inhibition potentials and mechanism. *Int J Biol Macromol* 2018;118:2216–23.
  47. Zhang J, Yang Y, Qian XK, et al. Design, synthesis, and structure–activity relationship study of pyrazolones as potent inhibitors of pancreatic lipase. *ChemMedChem* 2021;16:1600–4.
  48. Qian XK, Zhang J, Li XD, et al. Research progress on dipeptidyl peptidase family: structure, function and xenobiotic metabolism. *Curr Med Chem* 2021. DOI:10.2174/0929867328666210915103431.
  49. Zhang J, Qian XK, Song PF, et al. A high-throughput screening assay for dipeptidyl peptidase-IV inhibitors using human plasma. *Anal Methods* 2021;13:2671–8.
  50. Ma H, Qian X-K, Zhang J, et al. Accurate and sensitive detection of dipeptidyl peptidase-IV activity by liquid chromatography with fluorescence detection. *Anal Methods* 2020;12:848–54.
  51. Trott O, Olson AJ. AutoDock Vina: improving the speed and accuracy of docking with a new scoring function, efficient optimization, and multithreading. *J Comput Chem* 2010;31:455–61.
  52. Martinez-Gonzalez AI, Alvarez-Parrilla E, Díaz-Sánchez ÁG, et al. In vitro inhibition of pancreatic lipase by polyphenols: a kinetic, fluorescence spectroscopy and molecular docking study. *Food Technol Biotechnol* 2017;55:519–30.
  53. Wang L, Guan XQ, He RJ, et al. Pentacyclic triterpenoid acids in *Styrax* as potent and highly specific inhibitors against human carboxylesterase 1A. *Food Funct* 2020;11:8680–93.
  54. Qian XK, Zhang J, Song PF, et al. Discovery of pyrazolones as novel carboxylesterase 2 inhibitors that potently inhibit the adipogenesis in cells. *Bioorg Med Chem* 2021;40:116187.